Indian Journal of Ecology (2023) 50(2): 539-545
DOI: https://doi.org/10.55362/IJE/2023/3932

Manuscript Number: 3932
NAAS Rating: 5.79

Flood-Prone Area Mapping of Manu-Deo River Basin, Tripura using GIS and RS

Suman Debnath, Laxmi Narayan Sethi, Avinash Kumar, Nirmalya Kumar Nath[1] and Vinay Kumar Gautam[1]*

Department of Agricultural Engineering, Triguna Sen School of Technology
Assam University, Silchar-788 011, India
[1]Department of Soil and Water Engineering, CTAE, MPUAT, Udaipur-313 001, India
[*]E-mail: drvgautam95@gmail.com

Abstract: The present study has been undertaken for flood mapping integrating flood conditioning parameters through Analytical Hierarchal Process (AHP) utilizing Digital Elevation Models (DEMs) obtained by (Shuttle Radar Topography Mission) SRTM in a Geographic Information System (GIS) and Remote Sensing (RS) environment. The flood conditioning parameters such as elevation, slope, drainage density, flow accumulation, land-use land cover, annual rainfall, and stream order are selected for creating the thematic map using Digital Elevation Models (DEMs) obtained by (Shuttle Radar Topography Mission) SRTM and predicted area wise severity of flood hazard. The study revealed that around 13.43% of the study area and the cities like Kailashahar, Kumarghat, Pencharthal, and Kanchanpur having very little elevation, high drainage density and huge built-up were profoundly inclined to floods. However, the hilly regions or top-down portions (i.e., sources of the river) of the study area were spotted to be less prone to floods. This study will help to policy makers to recognize the hotspots of flood affected area to avoid any undesirable situation during monsoon season.

Keywords: AHP, Flood, DEM, SRTM, RS and GIS

Flood, landslides, earthquakes, tsunamis, drought, cyclones, volcanic eruptions, etc., are the different natural calamities that bring colossal disturbance to the ecosystem by demolishing various resources that disrupt a community's activities. Among all these natural calamities, flood is considered one of the most commonly occurring phenomena that strikes everywhere around the world (Das 2019, Kayastha et al 2013, Marchand et al 2009, Shen and Hwang 2019). Due to floods, a remarkable increase in disruption of economic activities, livelihood, and loss of life has been found over the past decades around the world (Gaume et al 2009).

India, due to its unique geo-climatic, and socio-economics is vulnerable in varying degrees to those natural calamities mentioned above and that they vary from region to region. In line with National Disaster Management Authority (NDMA) report of 2018, 58.6% of the Indian mainland is exposed to earthquakes of moderate to very high intensity; 12% of the land is susceptible to flood, and river erosion and a complete of 5,161 Urban Local Bodies (ULBs) are at the risk of urban flooding. The North-Eastern region of India is roofed by the mighty Brahmaputra-Barak River system and its tributaries. The southwest monsoon brings incessant rainfalls in this region which causes frequent floods (Trivedi et al 2021, Nath et al 2022). Avand et al (2020) identified the effects of changing climates and land uses over 20-18 years on flood probability using machine learning models by land change modeler (LCM) and Lars-WG software. Conicelli et al (2021) applying GIS and classic recharge methods determined groundwater availability and aquifer recharge in highly urbanized watersheds. Das (2020) generated a flood susceptibility map of the Western Ghat coastal belt combining multi-source geospatial data and analytical hierarchy process. MCDA has been broadly acknowledged as a significant procedure for dissecting complex choice issues which regularly include beyond reconciliation incommensurable rules (Malczewski 2006, Hwang and Lin 2012). The countless approach was created to generate flood-prone area maps such as adaptive neuro-fuzzy (Mahmound and Gan 2018), frequency ratio (de Santana et al 2021), analytical hierarchy process (Das 2018), statistical methods (Wang et al 2021), random forest (He et al 2022). The Analytical Hierarchy Process being one of the MCDA techniques is a subjective strategy where the system and its application depend on the specialist's information in assigning weights (Saaty 1980).

Flood mapping helps in deciding the protective measures that are to be taken to mitigate or to overcome the natural flooding phenomenon by promoting risk management, land use land cover management, flood forecasting (Kazakis et al 2015). Flooding is a multidimensional complex phenomenon

that causes flood mapping through ground survey and ariel observation to take time and also needs an experienced person. In recent years GIS/RS framework has significant attention from many researchers to investigate the expanse of flooded areas or computing natural calamities. The Geographic information system (GIS), is a framework that integrates, manages, and analyses the various types of input data, and systematizes the layer of information into visualization using maps and 3D scenes (Gautam et al 2021). This distinctive natural proficiency of GIS helps the user to frame smarter decisions by looking after the patterns, relationships, and solutions that are envisaged in the GIS environment by understanding the data in the form of a thematic map (Gautam et al 2023). Remotely-sensed data provide information by interpreting various features present on our planet and presenting it in the form of several digital images (Abdelkareem and El-baz 2017, Abdelkareem et al 2018). The combination of both GIS and RS techniques is extremely productive to generate flood-prone area mapping which comes up with substantial accuracy (Bates 2012, Nikoo et al 2016, Pradhan 2009, Rahmati et al 2016)

Almost every year, the cities nearby the Manu and Deo River get affected by floods which, causes hazards to human settlements as well as the economy. Understanding the flood dynamics by flood mapping is needed to predict floods and tackle future damages caused by floods. There are various ways to collect data, required for the study area but remote sensing high-resolution precise data are more effective than field survey. Currently, the GIS tool is commonly used for preparing and predicting flood hazard maps but applying (Analytical Hierarchal Process) AHP as a decision-making technique is still lacking in such study. Therefore, an attempt has been made to prepare a flood hazard map by applying AHP for the Manu-Deo River basin, Tripura by integrating flood conditioning parameters in a GIS environment. The principal objective of this study is to get familiar with and prepare flood hazard maps of the areas which are most prone to floods under the Manu-Deo River basin using GIS and RS which will help in taking protective measures to mitigate the destruction caused by the floods.

MATERIAL AND METHODS

Study area: The Manu-Deo River basin comes under three districts of Tripura i.e., Unakoti, North Tripura, and Dhalai, which is located between 23°15' N to 24°27' N latitude and 91°50' E to 92°18' E longitude (Fig. 1). The state of Tripura is blessed with well surface water resources. As per the report, 793 million cubic meters of water flow through ten major rivers annually. The Manu River originated from the Sakhan range which is northerly flowing through Kailashahar to

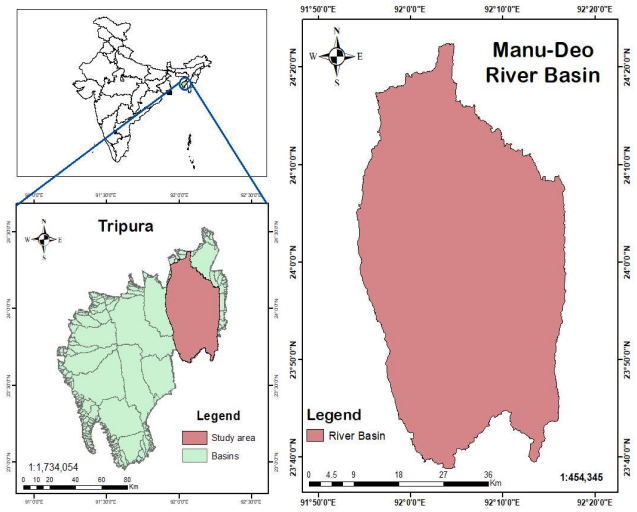

Fig. 1. Location of the Manu-Deo River basin

Bangladesh. An approximate length of 167 km makes it the. The longest river in Tripura. Whereas, 98 km long the Deo River move towards northward direction meets the Manu River via Kanchanpur valley and its origin is Jampui Hill.

Total area of the Tripura state is around 10,500 sq. km, have ten major rivers and other streams. Among them, the Manu-Deo River is the second largest river basin of Tripura covering 1,979 km^2 (18.36%) of the total basin area (The State of Environment in Tripura, 1989, CSME). The annual rainfall of the state varies from 1922 mm to 2855 mm. Humidity is usually high throughout the year; in the rainy season, it's over 85 percent while the average, maximum and minimum temperatures is 35.60°C and 4°C respectively. Rainfall is the major source of the generation of surface water in Tripura. It is noticed that the Manu-Deo River generates an annual flow of 170 million cubic meters of water which is 21.44% of the flow to total flow (The State of Environment in Tripura, 1989, CSME). Southwest monsoon contributes 60% of annual rainfall in this state, June being the highest rainfall receiving month followed by July. It was reported that 2542.5 mm as the highest mean annual rainfall in North Tripura district (98-104 days) and maximum (62-65 days) frequency of rainy days observed in the northern part of Dhalai, Unakoti, and North Tripura (IMD report 2020).

Sources of data: For flood-prone area mapping the Shuttle Radar Topographic Mission (SRTM), Digital Elevation Model (DEM) data was used (Hong et al 2018b). The SRTM, DEM data (Source: https://earthexplorer.usgs.gov/) of 30m spatial resolution was obtained from USGS Earth Explorer which helped in delineating the required river basin. To understand the current landscape of the study area Landsat 8 data of 1:50,000 scale for Land use land cover (LULC) map was acquired from USGS Earth Explorer. Pixel data of interannual

rainfall from 1998 to 2019 (Source: https://power.larc.nasa.gov/data-access-viewer/).

Analytic Hierarchy Process (AHP)

Implementation of AHP: The AHP involves the pair-wise comparison of the criteria assigned by the decision-makers and generates the weight of each criterion. The higher the score better the performance. Implementation of the AHP involves three successive steps: i) computing the vector if criteria weight, ii) computing the matric option scores, and iii) ranking the options.

Checking the consistency: For checking the consistency, the consistency index (CI) needs to find first. It can be computed as given below.

$$CI = \frac{\lambda_{max} - n}{n-1}$$

Where, λ_{max} is eigenvalue; n is the number of criteria or factors. The consistency ratio gives the required level of consistency, that is obtained using CI and RI.

$$CR = \frac{CI}{RI}$$

Where, CR is the consistency ratio; CI is the consistency index, and RI is the random index. The acceptable consistent ratio (CR) value should be below 0.1 (i.e., R < 0.1) otherwise it will call as inconsistent. The RI value that is to be used is according to Table 1.

To prepare thematic layers, different geo-spatial data have been collected from their respective sources for the study area using ArcGIS 10.3. The final flood-prone area map was prepared by integrating all the factors in the (Geographic Information System) GIS environment with an allocated weighted value of the respective parameters. Whereas, the hierarchical classification based on the flood vulnerability was done by the Analytical Hierarchal Process (AHP) Technique shown in Figure 2.

RESULTS AND DISCUSSION

Elevation: The elevation (i.e., distance above the sea level) of the study area varies from 18m to 940m which were classified into six classes Figure (3a). Elevation with a higher value as steeper topography, resulting in less vulnerability to floods.

Slope: As the slope of an area goes on decreasing the infiltration rate starts increasing as a result surface runoff decrease and it creates a flooding situation where the water starts overflowing and stops the water from reaching the river channel. Hence, the higher the topographic gradient lesser the probability of occurrence of flood. The five classes of slopes that have been categorized depending on their susceptibility to inundating: very low, low, medium, high, very high. Breaking values were taken based on experts' knowledge, local information (Fig. 3b).

Drainage density: The areas with extremely high river discharge led to an increase in the occurrence of floods, thus it's a crucial factor in flood mapping (Mahmoud and Gan 2018, Ogden et al 2011). The drainage density was between 0 to 2.5 km/km^2, which has been classified into five classes (Fig. 3c).

Flow accumulation: Flow accumulation indicates the accumulated weight of the watershed flowing through the outlet toward the downslope. It is a very important factor that has a great influence on flood mapping. Increasing the value of flow accumulation leads to an increase in flood-prone areas (Lehner et al 2006). This flow accumulation map is generated by flood accumulation tools in ArcGIS and categorized into five classes based on natural breaks. It is useful in the generation of stream networks (Fig. 3d).

Land use land cover: Land use land cover adversely affect the flood propagation and varies from less impervious land to more impervious land, on the other way the forest has a big capacity to intercept the rainfall as compared to vegetation

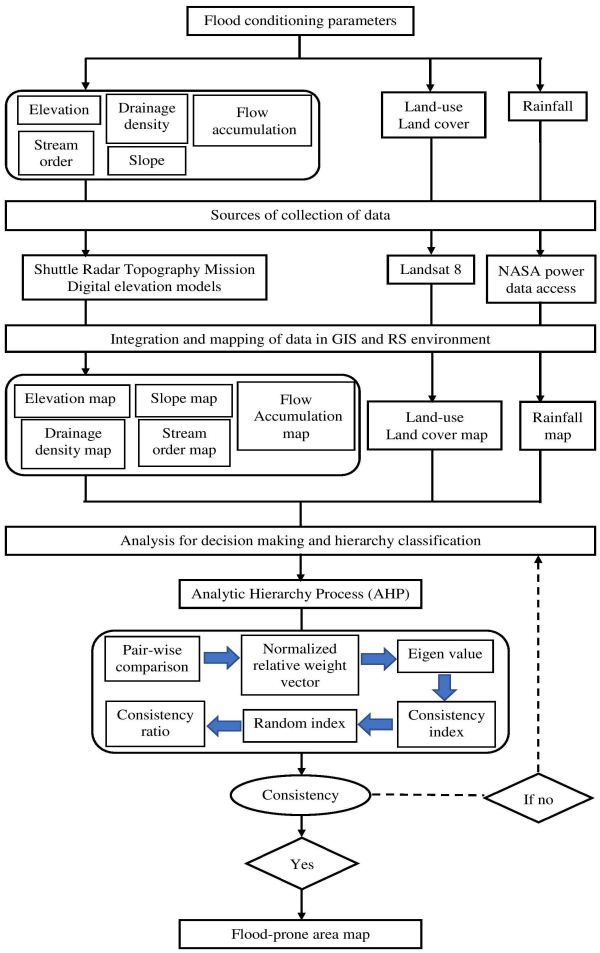

Fig. 2. Flow chart of flood-prone area mapping for the Manu-Deo River basin

land or scrubland. Land use pattern has a strong tendency to control the flooding consistency (Benito et al 2010, Garcia-Ruiz et al 2008). Transformation in land use can lead to an increase in the occurrence of floods in an area (Beckers et al 2013). The prepared LULC map in this study is of eight land use classes i.e., Deciduous Forest, cropland, built-up land, mixed forest, shrubland, waterbodies, plantation, evergreen forest (Fig. 4a).

Rainfall: It is evident that rainfall has a great impact on river flooding as many have established the relationship between flood occurrence and rainfall (Goel et al 2000, Hong et al 2018a, 2018b, Zhao et al 2018). The map prepared here was based on of last 20 years' annual rainfall data which were categorized into five classes based on the amount of rainfall received by different stations within the study area and maximum or minimum rainfall found to be 1869 or 1790 mm/year respectively (Fig. 4b).

Stream order: Water starts overflowing when the amount of water drained through the steam gets beyond its capacity. Usually, a flood occurs when a greater number of streams collect water from different areas and passes through the mainstream i.e., higher the level of branching in a river system leads to the increase in the occurrence of floods, and areas nearby the river mouth are more prone to the flood as compared to areas top-down surrounding areas. The stream network system of the study area was divided into five orders Figure 4(c).

Consistency checking: The numerical values of the pairwise comparison matrix shown in Table 2 give the qualitative evaluations of the relative importance between

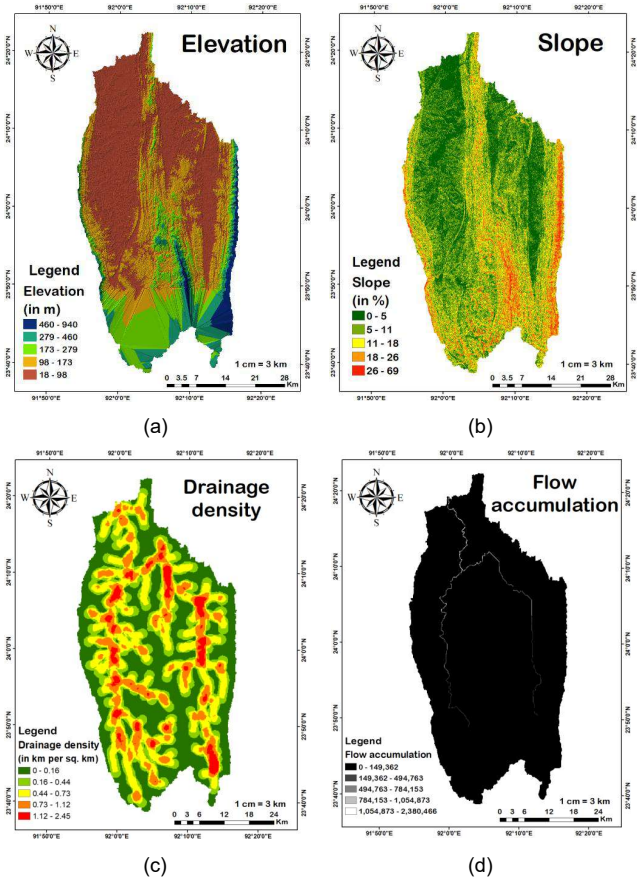

Fig. 3. Thematic maps for flood conditioning parameters, (a) Elevation, (b) Slope, (c) Drainage density (d) Flow accumulation of the study area

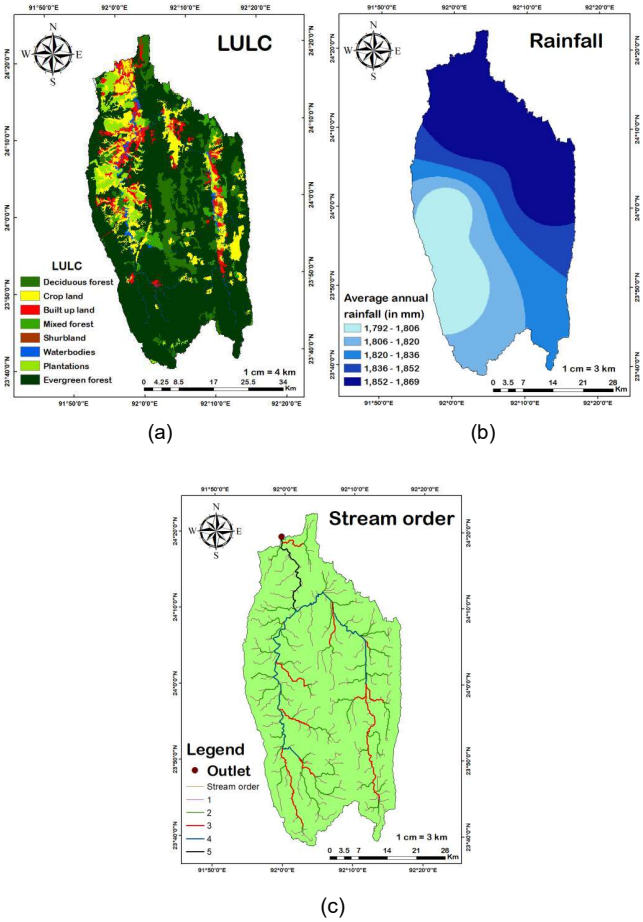

Fig. 4. Thematic maps for flood conditioning parameters (a) LULC, (b) Rainfall, (c) Stream order of the study area

Table 1. Values of the Random Index (RI)

n	1	2	3	4	5	6	7	8	9	10
RI	0	0	0.58	0.89	1.21	1.24	1.32	1.41	1.45	1.49

Source: Saaty 1980

the two parameters. The relation between numerical values and high respective importance was: 1, 3, 5, 7, and 9 represents the equally slightly more, more, strongly, and absolutely more important respectively whereas less significant variable was allotted by reciprocal of that number (Saaty 2004, Kandilioti and Makropoulos 2012), The normalized matrix values whose average (along the rows) gives that criteria weight value of each parameter (Table 3). The average of the ratio of weighted sum value to the criteria weight calculated. It represents the value of the eigenvector (Table 4).

λ_{max}= (7.79 + 7.97 + 7.57 + 7.40 + 7.80 + 6.75 + 8.00)/7 = 7.60

Applying the following equation, consistency index was calculated by computing the average eigenvalue and the number of criteria that have been used in the study.

$$CI = \frac{7.60 - 7}{7 - 1} = 0.1$$

Using the following equation, consistency ratio was simplified by considering 1.32 as a random index value for seven criteria.

$$CR = \frac{0.10}{1.32} = 0.08$$

The obtained value of CR as 0.08<0.1 signified that the weighted value allocated to the respective parameters like elevation, slope, drainage density, flow accumulation, land-use land cover, rainfall, and stream order as 0.37, 0.26, 0.15, 0.10, 0.05, 0.04 and 0.02 respectively were consistent.

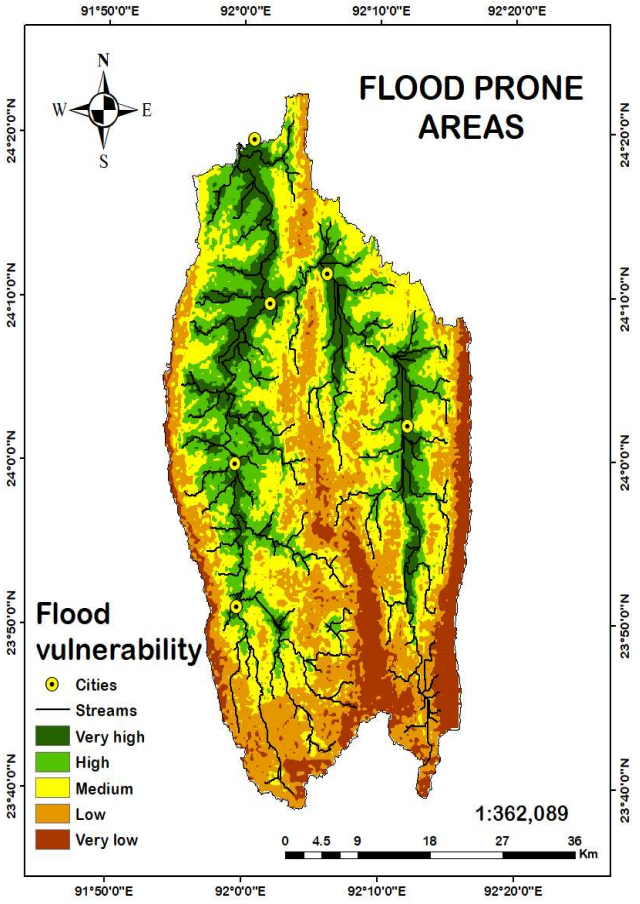

Fig. 5. Flood-prone area mapping of the Manu-Deo River basin

Table 2. Pairwise of comparison matrix of all the parameters

Parameters	Elevation	Slope	Drainage density	Flow accumulation	LULC	Rainfall	Stream order
Elevation	1	2	4	5	7	8	9
Slope	1/2	1	3	4	6	7	8
Drainage density	1/4	1/3	1	2	4	6	7
Flow accumulation	1/5	1/4	1/2	1	3	4	5
LULC	1/7	1/6	1/4	1/3	1	2	4
Rainfall	1/8	1/7	1/6	1/4	1/2	1	3
Stream order	1/9	1/8	1/7	1/5	1/4	1/3	1

Table 3. Criteria weight of all the parameters for AHP technique

Parameters	Elevation	Slope	Drainage density	Flow accumulation	LULC	Rainfall	Stream order	Criteria weight
Elevation	0.43	0.50	0.44	0.39	0.32	0.28	0.24	0.37
Slope	0.21	0.25	0.33	0.31	0.28	0.25	0.22	0.26
Drainage density	0.11	0.08	0.11	0.16	0.18	0.21	0.19	0.15
Flow accumulation	0.09	0.06	0.06	0.08	0.14	0.14	0.14	0.10
LULC	0.06	0.04	0.03	0.03	0.05	0.07	0.11	0.05
Rainfall	0.05	0.04	0.02	0.02	0.02	0.04	0.08	0.04
Stream order	0.05	0.03	0.02	0.02	0.01	0.01	0.03	0.02

Table 4. Determination of eigen value

Parameters	Elevation	Slope	Drainage density	Flow accumulation	LULC	Rainfall	Stream order	Weighted sum	Criteria weight	Weighted sum/Criteria weight
Elevation	0.37	0.53	0.60	0.50	0.38	0.30	0.21	2.88	0.37	7.79
Slope	0.19	0.26	0.45	0.40	0.33	0.27	0.18	2.07	0.26	7.97
Drainage density	0.09	0.09	0.15	0.20	0.22	0.23	0.16	1.14	0.15	7.57
Flow accumulation	0.07	0.07	0.07	0.10	0.16	0.15	0.11	0.74	0.10	7.40
LULC	0.05	0.04	0.04	0.03	0.05	0.08	0.09	0.39	0.05	7.80
Rainfall	0.05	0.04	0.02	0.02	0.03	0.04	0.07	0.27	0.04	6.75
Stream order	0.04	0.03	0.02	0.02	0.01	0.01	0.02	0.16	0.02	8.00

All the seven multi-sources environmental criteria that were considered in this study were merged to generate a flood-prone area map. The preferences given to the flood condition parameters were based on the weighted value generated by the AHP technique. The resulting map prepared by overlaying was classified into five classes dependent on the natural breaking method. They are as follows: very high, high, medium, low, and very low. After calculating the area under flood-prone it was found that 282.96 km^2 (13.43%), 450.40 km^2 (21.38%), 596.70 km^2 (28.32%), 531.92 km^2 (25.25%), and 244.77 km^2 (11.62%) of the total area were corresponded to very high, high, medium, low, and very low vulnerable to floods respectively (Fig. 5). The city of Kailashahar, Kumarghat, Manu, Pecharthal, Kanchanpur across the basin come under very high flood-prone zone including some portions of the cropland or flat land areas nearby the main streams. On the other hand, hilly areas or top-down portions (i.e., sources of the river) were spotted to be less prone to floods. The areas with very little elevation, zero slopes, high drainage density, excessive-high flow accumulation, and huge built-up areas are very highly prone to floods.

CONCLUSION

The flood-prone area map of the Manu-Deo River basin was prepared using GIS and RS applying AHP techniques as an effective tool for complex decision making. The areas with lower elevation, slope, and high flow accumulation are very highly prone to floods. Additionally, the intensity of floods was observed to be very high in the areas with the highest number of recorded historical flooding events within the study area. There is the lowest percentage of areas where chances of affected areas with floods are very less. The AHP model used was accurate and reliable when used together with GIS and RS. Hence, the map of flood-prone areas presented in this paper can be used in preparing flood maps of other areas and also may help the organizational bodies, engineers, policymakers, builders, service providers in tackling floods in the Manu-Deo River basin.

REFERENCES

Abdelkareem M and El-Baz F 2017. Remote sensing of paleodrainage systems west of the Nile River, Egypt. *Geocarto International* **35**: 1-10.

Abdelkareem M, Akrby A, Fakhry M and Mostafa M 2018. Using of remote sensing and aeromagnetic data for predicting potential areas of hydrothermal mineral deposits in the central eastern desert of Egypt. *Remote Sensing Applications: Society and Environment* **7**: 1-13.

Avand M, Moradi H and Iasboyee RM 2020. Using machine learning models, remote sensing and GIS to investigate the effects of changing climates and land uses on flood probability. *Journal of Hydrology* 1-49.

Bates PD 2012. Integrating remote sensing data with flood inundation models: How far have we got? *Hydrological Processes* **26**(16): 2515-2521.

Beckers A, Dewals B, Erpicum S, Dujardin S, Detrembleur S, Teller J, Pirotton M and Archambeau P 2013. Contribution of land use changes to future flood damage along the river Meuse in the Walloon region. *Natural Hazards and Earth System Sciences* **13**: 2301-2318.

Benito G, Rico M, Sanchez-Moya Y, Sopena A, Thorndycraft VR and Barriendos M 2010. The impact of late Holocene climate variability and land-use change on the flood hydrology of the Guadalentin River, southeast Spain. *Global and Planetary Change* **70**: 53-63.

Conicelli B, Hirata R, Galvão P, Bernardino M, Simonato M, Abreu MC, Aranda N and Terada R 2021. Determining groundwater availability and aquifer recharge using GIS in a highly urbanized watershed. *Journal of South American Earth Sciences* **106**: 103093.

Das S 2018. Geographic information system and AHP based flood hazard zonation of Vaitarna basin, Maharastra, India. *Arabian Journal of Geosciences* **11**: 576.

Das S 2019. Geospatial mapping of flood susceptibility and hydro-geomorphic response to the flood in Ulhas basin, India. *Remote Sensing Application: Society and Environment* **14**: 60-74.

Das S 2020. Flood susceptibility mapping of the Western Ghat coastal belt using multi-source geospatial data and analytical hierarchy process (AHP). *Remote sensing Applications: Society and Environment* **20**: 1-17.

De Santana RO, Delgado RC and Schiavetti A 2021. Modeling susceptibility to forest fires in the Central Corridor of the Atlantic Forest using the frequency ratio method. *Journal of environmental management* **296**: 113343.

Desalegn H and Mulu A 2020. Flood vulnerability assessment using GIS at Fetam watershed, upper Abbay basin, Ethiopia. *Heliyon* **6**: 1-14.

García-Ruiz JM, Regüés D, Alvera B, Lana-Renault N, Serrano-Muela P, Nadal-Romero E, Navas A, Latron J, Martí-Bono C and Arnáez J 2008. Flood generation and sediment transport in experimental catchments affected by land use changes in the central Pyrenees. *Journal of Hydrology* **356**: 245-260.

Gaume E, Bain V, Bernardara P, Newinger O, Barbuc M, Bateman A, Blaskovicova L, Bloschl G, Borga M and Dumitrescu A 2009. A compilation odd data on European flash floods. *Journal of Hydrology* **367**: 70-78.

Gautam VK, Kothari M, Singh PK and Yadav KK 2021. Determination of geomorphological characteristics of Jakham River Basin using GIS technique. *Indian Journal of Ecology* **48**(6): 1627-1634.

Gautam VK, Pande CB, Kothari M, Kumar Singh P, Agrawal A 2023. Exploration of groundwater potential zones mapping for hard rock region in the Jakham river basin using geospatial techniques and aquifer parameters. *Advances in Space Research* **71**(6): 2892-908.

Goel NK, Kurothe RS, Mathur BS and Vogel RM 2000. A derived flood frequency distribution for correlated rainfall intensity and duration. *Journal of Hydrology* **228**: 56-67.

Halgamuge NM and Nirmalathas T 2017. Analysis of large food events: based on flood data during 1985-2016 in Australia and India. *International Journal of Disaster Risk Reduction* 1-18.

He S, Wu J, Wang D and He X 2022. Predictive modeling of groundwater nitrate pollution and evaluating its main impact factors using random forest. *Chemosphere* **290**: 133388.

Hong H, Panahi M, Shirzadi A, Ma T, Liu J, Zhu A and Chen W 2018a. Flood susceptibility assessment in Hengfeng area coupling adaptive neuro-fuzzy inference system with genetic algorithm and differential evolution. *Science of the Total Environment* **621:** 1124-1141.

Hong H, Tsangaratos P, Ilia I, Liu J, Zhu A and Chen W 2018b. Application of fuzzy weight of evidence and data mining techniques in construction of flood susceptibility map of Poyang country, China. *Science of the Total Environment* **6**: 575-588.

Hwang CL and Lin MJ 2012. *Group discussion making under multiple criteria: Methods and applications.* **281**: Springer Science and Business Media.

Kandilioti G and Makropoulos C 2012. Preliminary flood risk assessment. The case of Athens. *Natural Hazards* **61**: 441-468.

Kayastha P, Dhital MR and De Smedt F 2013. Application of analytical hierarchy process (AHP) for landslide susceptibility mapping: A case study from the Tinau watershed, west Nepal. *Computers and Geosciences* **52**: 398-408.

Kazakis N, Kougias I and Patsialis T 2015. Assessment of flood hazard areas at a regional scale using an index-based approach and analytical hierarchy process: Application in rhodope-evros region, Greece. *Science of the Total Environment* **538**: 555-563.

Lehner B, Döll P, Alcamo J, Henrichs T and Kaspar F 2006. Estimating the impact of global change on flood and drought risks in Europe: A continental, integrated analysis. *Climatic Change* **75**: 273-299.

Mahmound SH and Gan TY 2018. Multi-criteria approach to develop flood susceptibility maps in arid regions of Middle East. *Journal of Cleaner Production* **196:** 216-229.

Malczewski J 2006. GIS-based multicriteria decision analysis: A survey of the literature. *International Journal of Geographical Information Science* **20**: 703-726.

Marchand M, Buurman J, Pribadi A and Kurniawan A 2009. Damage and causalities modelling as part of a vulnerability assessment for tsunami hazards: a case study from Aceh, Indonesia. *Journal of Flood Risk Management* **2**: 120-131.

Mojaddadi H, Pradhan B, Nampak H, Ahmad N and Ghazali AHB 2017. Ensemble machine learning-based geospatial approach for flood risk assessment using multi-sensor remote sensing data and GIS. *Geomatics Natural Hazard and Risk* **8**: 1080-1102.

Nath NK, Agrawal A, Gautam VK, Kumar A and Das P 2022. Morphometric evaluation of Ranikhola watershed in Sikkim, India using geospatial technique. *Environment Conservation Journal* **23**(3):273-84.

Nikoo M, Ramezani F, Hadzima-Nyarko M, Nyarko EK and Nikoo M 2016. Flood-routing modelling with neural network optimized by social-based algorithm. *Natural hazards* **82**: 1-24.

Nithyay SE, Blessy J and Viji R 2021. Flood vulnerability mapping using frequency ratio model and dempster shafer theory: A case study on devikulam and udumbanchola taluks of Ldukki district, Kerala, India. *Indian Journal of Ecology* **48**: 982-989.

Ogden FL, Raj Pradhan N, Downer CW and Zahner JA 2011. Relative importance of impervious area, drainage density, width function, and subsurface storm drainage on flood runoff from an urbanized catchment. *Water Resources Research* **47**, W12503, doi :10.1029/2011WR010550.

Pradhan B 2009. Flood susceptible mapping and risk area delineation using logistic regression, GIS and remote sensing. *Journal of Spatial Hydrology* **3**: 1-18.

Rahmati O, Pourghasemi HR and Zeinivand H 2016. Flood susceptibility mapping using frequency ratio and weights-of-evidence models in the Golestan Province, Iran. *Geocarto International* **31**: 42-70.

Ramola M, Nayak PC, Venkatesh B and Thomas T 2021. Dam break analysis using hec-ras and flood inundation modelling for Pulichinatala Dam in Andhra Pradesh, India. *Indian Journal of Ecology* **48**: 620-626.

Saaty TL 1980. *The Analytic* Hierarchy Process. McGraw-Hill, New York.

Saaty TL 2004. Decision making: The analytic hierarchy and network processes (AHP/ANP). *Journal of Systems Science and Systems Engineering* **13**: 1-35.

Shen G and Hwang SN 2019. Spatial-Temporal snapshots of global natural disaster impacts Revealed from EM_DAT for 1900-2015. Geomatics, *Natural Hazards and Risk* **10**: 912-934.

Trivedi A, Galkate RV, Gautam VK, Pyasi SK 2011. Development of RRL AWBM model and investigation of its performance, efficiency and suitability in Shipra River Basin. *Journal of Soil and Water Conservation* **20**(2):160-167.

Vaishnavi B, Yarrakula K and Karthikeyan J 2020. Flood inundation mapping of lower Godavari riverbasin using remote sensing and GIS. *Indian Journal of Ecology* **47**: 30-35.

Received 06 December, 2022; Accepted 07 March, 2023